

Article

Rheological and Frictional Properties of Lithium Complex Grease with Graphene Additives

Yanshuang Wang^{1,2}, Xudong Gao^{1,2}, Jianghai Lin^{1,2,*} and Pu Zhang^{1,2}

¹ School of Mechanical and Automotive Engineering, Qilu University of Technology (Shandong Academy of Sciences), Jinan 250353, China; wys2021@qlu.edu.cn (Y.W.); 201601011161@stu.qlu.edu.cn (X.G.); 10431200115@stu.qlu.edu.cn (P.Z.)

² Shandong Institute of Mechanical Design and Research, Jinan 250031, China

* Correspondence: ljh2021@qlu.edu.cn

Abstract: Few-layer graphene (FLG) was added as a nano-additive to lithium complex grease (LCG) to explore the influence of FLG on the microstructure, viscoelasticity, friction and wear properties of LCG. Studies have found that the addition of FLG makes the microstructure of the thickener more compact, which in turn leads to an increase in the viscoelasticity of LCG. FLG additives can improve the viscosity-temperature properties of the grease and change the elastic deformation response to temperature changes. Among the temperatures selected in this article, the effect of graphene is more obvious at 70 °C. During the friction process, a proper amount of FLG can quickly form a boundary film and is not easily damaged, thereby optimizing the friction and wear performance of LCG.

Keywords: few-layer graphene; lithium complex grease; viscoelasticity; friction and wear properties



Citation: Wang, Y.; Gao, X.; Lin, J.; Zhang, P. Rheological and Frictional Properties of Lithium Complex Grease with Graphene Additives. *Lubricants* **2022**, *10*, 57. <https://doi.org/10.3390/lubricants10040057>

Received: 10 March 2022

Accepted: 29 March 2022

Published: 1 April 2022

Publisher's Note: MDPI stays neutral with regard to jurisdictional claims in published maps and institutional affiliations.



Copyright: © 2022 by the authors. Licensee MDPI, Basel, Switzerland. This article is an open access article distributed under the terms and conditions of the Creative Commons Attribution (CC BY) license (<https://creativecommons.org/licenses/by/4.0/>).

1. Introduction

Grease is an indispensable part of bearings [1]. Recently, lubricating grease has received extensive attention among engineers and scientists in academia as a result of its complex and unique rheological properties. Generally, a series of rheological parameters are selected to ascertain the rheological properties of grease in both qualitative and quantitative terms. Lithium-based grease is one of the most common greases, and the factors affecting its rheology have attracted the attention of many scholars. Enhui Zhang et al. [2] prepared four lithium-based greases with paraffin oil, naphthenic oil, poly- α -olefin and polyol ester, respectively, and studied the influence of base oil on the rheological and frictional properties of lithium-based greases. It was found that naphthenic oil-based grease exhibited the best colloidal stability, and the thickener fibers in the polyethylene-based grease show a relatively flat network. Compared with the planar network structure, the lithium soap fiber with a three-dimensional entangled structure has a stronger friction reducing ability. Xiaoqiang Fan et al. [3] studied the influence of different thickeners on the friction characteristics of greases. They found that the excellent lubricating performance of the grease is mainly attributed to the properties and structure of the thickener and the synergistic effect of the grease film composed of sulfate and complex oxides and the tribochemical reaction film. Although additives account for a relatively low proportion of the grease by mass or volume, they have a greater influence on the rheological properties thereof.

Many nano-materials can be used as solid lubricants and can also be used as additives in lubricating oils and greases. Nikhil Kumar et al. added nanoparticles of Talc [4] and PTFE particles [5] into lithium-based grease to study its rheology and friction properties. It is found that the smaller the size of the additive material, the better the friction performance of the lithium-based grease. Compared with other shapes, the spherical particles can improve the friction performance of the lithium-based grease. Few-layer graphene (FLG) is a kind of nano material with many excellent properties. It has good thermal conductivity and can significantly improve the cooling performance of lubricants [6]. As a coating, it can improve

the corrosion resistance of metals [7]. After investigation, it is found that as a lubricating additive, the ease of the peeling of the FLG facilitates the formation of a boundary film under a frictional load, which not only prevents direct contact between friction pairs, and improves the flexibility and adaptive ability of the friction interface, but, as the FLG spacing in the boundary film is relatively large, and the van der Waals force between the layers is low, this can promote lubrication by reducing the energy barrier between layers [8–10].

Some studies have found that adding FLG to lubricating oil can significantly improve the lubricating performance and friction performance of the lubricating oil; the friction coefficient (COF), wear scar diameter (WSD), and wear volume have been significantly reduced [11–16]. Tiancheng Ouyang et al. [17] added FLG to PAO6 base oil. Under low speed and heavy load conditions (4.2 mm/s and 1.0 GPa contact pressure), COF and wear volume loss can be reduced by as much as 29.1% and 55%, respectively.

For non-Newtonian greases, FLG also has a significant effect on its rheology. Mohamed et al. [18] added FLG and multi-walled carbon nanotubes to a composite calcium-based grease to make a mixed calcium nano-grease, and conducted rheological experiments using the Brookfield DV-III programmable rheometer, and found that the shear stress and viscosity increased with the addition of nano-additives. In recent years, researchers have added FLG to lithium grease to study the friction characteristics, and found that the addition of FLG has improved their anti-wear and anti-friction properties. Zhanjun Li et al. [19] added FLG to lithium-based grease and found that when the FLG content is 0.1%, the COF reduction rate is the largest, and the wear scar diameter (WSD) is the smallest, and FLG has the most obvious effect under a larger load and lower speed. The main component of the chemical reaction film on the friction surface of pure lithium grease is Fe_3O_4 . After adding FLG, the main components of the boundary film become Fe_2O_3 and adsorbed FLG. Jin Zhang et al. [20] found through research that, compared with pure lithium grease with an FLG content of 2 wt%, the average friction coefficient is reduced by 27%, and the solder joint and load wear index are 1.6 and 1.4 times that of pure lithium grease, respectively. Tiancheng Ouyang et al. [21] found that the addition of FLG can significantly improve the anti-friction and anti-wear ability of the grease, thereby making the wear surface smoother. In particular, compared with lithium grease, the wear amount and COF of lithium grease containing 0.3 wt% FLG can be reduced by 52.0% and 20.3%, respectively. Ruslan Aziev et al. [22] found that after FLG was added to LCG, the tribochemical reaction between 12-hydroxystearate molecules and the surface of FLG occurred, resulting in an increase in the welding load and a decrease in the WSD. Bo Lin et al. [23] added graphene to lithium-based grease to study its tribological behavior under three operating conditions: slow moving heavy load, medium load speed and high speed light load. The study found that under different working conditions, the optimum content of graphene that makes the grease with the best anti-wear and anti-friction ability is different.

FLG composite materials can also improve the lubricating ability and anti-wear and anti-wear ability of lithium-based greases. Jin, Bao et al. [24] developed a $\text{Mn}_3\text{O}_4/\text{FLG}$ ($\text{Mn}_3\text{O}_4\#\text{G}$) nanocomposite and used it as a nano-additive for lithium-based grease. The study found that under the conditions of 100 °C and 150N load, when the concentration of $\text{Mn}_3\text{O}_4\#\text{G}$ is 0.03 wt%, COF and wear scar depth can be reduced by 35% and 76%, respectively, and the addition of $\text{Mn}_3\text{O}_4\#\text{G}$ enhances the ability of lithium-based grease to withstand high temperatures. Liu Xiaolong et al. [25] obtained FLG oxide by Hummers oxidation method and added it to lithium grease. The study found that FLG oxide as a grease additive can effectively reduce COF, reduce wear, extend lubrication time, and improve lubricating performance. FLG can also enhance its lubricating ability, anti-wear and anti-wear ability for other types of grease [26,27].

Most of the aforementioned projects involved the investigation of the influence of FLG additives on the viscosity of lubricating oils and greases, however, there is a lack of research on the influence of FLG additives on other rheological parameters such as yield strength, cross-stress, and elastic modulus, and there is no literature comprehensively covering the rheological properties parameters of greases with different FLG contents across a range of

temperatures. There is no relevant report on research into the influence mechanism of FLG additives on the rheological properties and friction properties of LCG. In the present study, FLG was used as an additive to prepare LCG. Amplitude scanning and shear scanning experiments were conducted using a rheometer to measure the rheological properties of LCG containing different amounts of FLG at different temperatures. The SRV-4 friction tester was used to conduct friction experiments on LCG to study the influence of the content of FLG on the tribological behavior of LCG. A scanning electron microscope (SEM) was employed to characterize the micro-morphology of LCG, analyze the influence of FLG on the micro-morphology of LCG, and reveal the mechanism of the influence of FLG additives on the rheological and friction properties of LCG.

2. Materials and Methods

2.1. Material Processing and Sample Preparation

The thickener material of the LCG is 12-hydroxystearic acid (China Petrochemical Corporation Tianjin Branch, Tianjin, China) with the contents of 15%, and the base oil is mineral oil and PAO oil (China Petrochemical Corporation Tianjin Branch, Tianjin, China) with a viscosity of 220 cst. Lithium hydroxide aqueous solution (China Petrochemical Corporation Tianjin Branch, Tianjin, China) is added for saponification reaction to generate LCG. The additive is Changzhou sixth element graphene SE1231 (Changzhou Sixth Element Materials Technology Co., Ltd., Changzhou, China). The SE1231 graphene is a black powder, and the median particle size D_{50} is less than 10.0 μm (equivalent spherical diameter). Taking 50 g of mineral oil and PAO oil, we added a certain amount of FLG, mixed them and placed it in an ultrasonic cleaning machine for 2 h. We added 350 g of the LCG into the aforementioned mineral oil and PAO oil containing FLG to prepare an FLG mixed LCG with mass fractions of 0.5, 1, and 2 wt%. We used an SDF1100-type dispersing sand mill (Suzhou Qile Electronic Technology Co., Ltd., Suzhou, China) to mix and grind the specimens at 900 rpm for 2 h, so that the FLG is uniformly mixed within the LCG.

2.2. Experimental Procedure

The MCR302 rheometer (Anton Paar Instruments, Graz, Steiermark, Austria) was used to measure the rheological properties of the four LCG specimens. The experiment is divided into two parts: amplitude scan and shear scan. Lubricating grease is a viscoelastic fluid, and the shear scan uses the rheometer-rotation mode with the cp25-1 cone-plate test system with a diameter of 25 mm and an angle of 1.0° ; the amplitude sweep uses the rheometer-oscillation mode with the pp25 parallel plate test system with a diameter of 25 mm. The experiment was conducted at three temperatures, respectively 30 $^\circ\text{C}$, 70 $^\circ\text{C}$ and 130 $^\circ\text{C}$ (± 0.1 $^\circ\text{C}$). The rotation mode used in shear scanning is to apply strain or stress with continuous rotation in the same direction to obtain a constant shear-strain rate (i.e., a steady-state test). The controlled shear-strain rate (CSR) rotation mode is selected and the shear-strain rate $\dot{\gamma}$ (s^{-1}) is set to obtain a certain shear strength τ (Pa) of the grease. The oscillation mode used in amplitude sweeps is a reciprocating mode of oscillation designed to apply constant strain or stress (i.e., a dynamic test). The controlled strain (CS) mode of oscillation is selected, and the shear strain is set to obtain a certain shear strength τ (Pa) of the grease in an oscillating state of strain. Before each test, pre-shearing is applied for between five and fifteen minutes to eliminate the residual stress in the grease.

The SRV-4 friction and wear tester (Optimol Instruments, Munich, Germany) was used to measure the friction properties of the four LCG specimens. The test steel ball has an accuracy of G10, a diameter of 10.318 mm, and a set load of 90 N. According to the Hertz formula, the working stress is 2.04 GPa. The test adopts a reciprocating mode with a frequency of 10 Hz and an amplitude of four mm. The test temperature was set to 30 $^\circ\text{C}$ and test time to 0.5 h. COF curves of the four LCG were obtained. Three friction tests were performed for each grease. The MIT300 metallurgical microscope (Chongqing Auto Optical Instrument Co., Ltd., Chongqing, China) was used to measure the WSD on the steel ball after each test.

3. Results

3.1. Effect of FLG on the Microstructure of LCG

Figure 1 shows the FT-IR spectra of LCG with different content of FLG. The IR bands appearing at $2890\text{--}2960\text{ cm}^{-1}$ and 1580 cm^{-1} were ascribed to C=O groups, respectively. The bands appearing at 1460 and 1375 cm^{-1} were ascribed to the stretching vibrations of C–H and O–H groups, respectively. For the bands appearing at $3500\text{--}4000\text{ cm}^{-1}$, as the FLG content increases, the fluctuation becomes more obvious, indicating that they were ascribed to the stretching vibration of the C–C group in FLG.

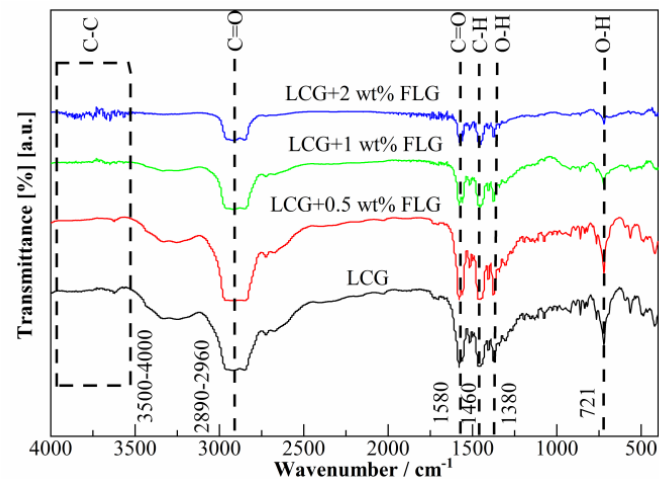


Figure 1. FT-IR spectra of LCG specimens.

Figure 2 shows SEM micrographs of the LCG with the base oil washed away and the LCG with 2 wt% FLG added. Figure 2a demonstrates that the microstructure of the LCG thickener is a fiber structure; in Figure 2b, 2 wt% FLG is added to the LCG, and it is found that the thickener fiber structure is wound on the surface of FLG; since FLG is polar, it will be preferentially adsorbed on the thickener of the same polarity when added, which increases the polarity of the thickener. Under the condition that the polarity of the base oil remains unchanged, this leads to a gap between the base oil and the thickener. The difference in polarity is greater, and the thickening agent is not easily dispersed in the base oil, resulting in a denser thickening agent.

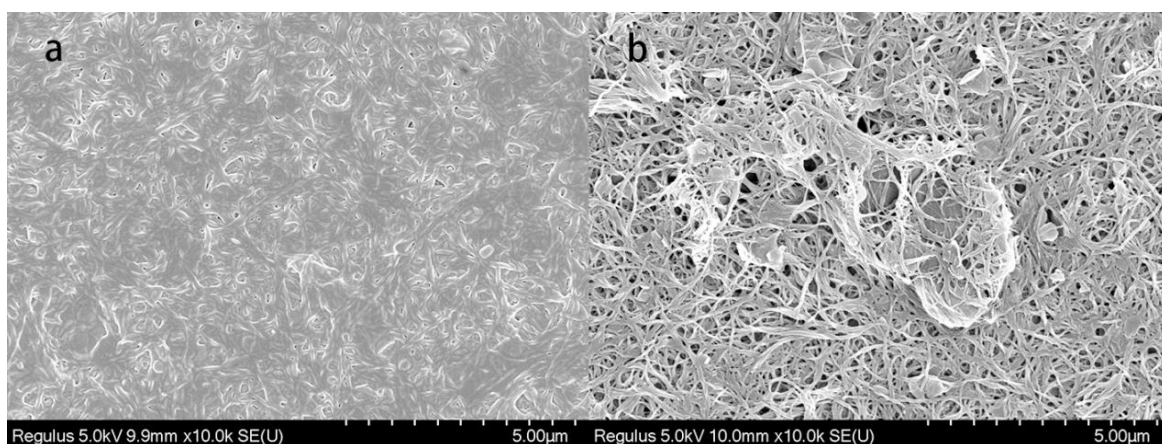


Figure 2. SEM micrograph of LCG specimens. (a) LCG; (b) LCG with 2 wt% FLG.

3.2. Effect of FLG on the Viscoelasticity of LCG

Grease is a semi-solid material that is both viscous and elastic. To study the viscoelastic properties of grease, the complex modulus is introduced [28]. The complex modulus of grease (G^* , Pa) can be described by example (1):

$$G^* = G' + i G'' \quad (1)$$

where, G' is the storage modulus, which represents the energy stored by the elastic deformation of the grease, Pa; G'' denotes the loss modulus, which represents the energy dissipated during viscous deformation of the grease, Pa.

A rheometer was used to perform amplitude sweep experiments on four LCG samples in oscillation mode, and the relationship between storage modulus G' and loss modulus G'' with shear strain at three test temperatures (30 °C, 70 °C and 130 °C) was obtained (Figure 3). With the increase in shear stress, the storage modulus G' continuously decreases, while the loss modulus G'' increases, before finally converging at the flow point. The stress corresponding to the flow point is called the cross-stress. Beforehand, the elasticity of the LCG plays a dominant role, and thereafter, the LCG exhibits flow characteristics, and the viscosity of the LCG plays a dominant role.

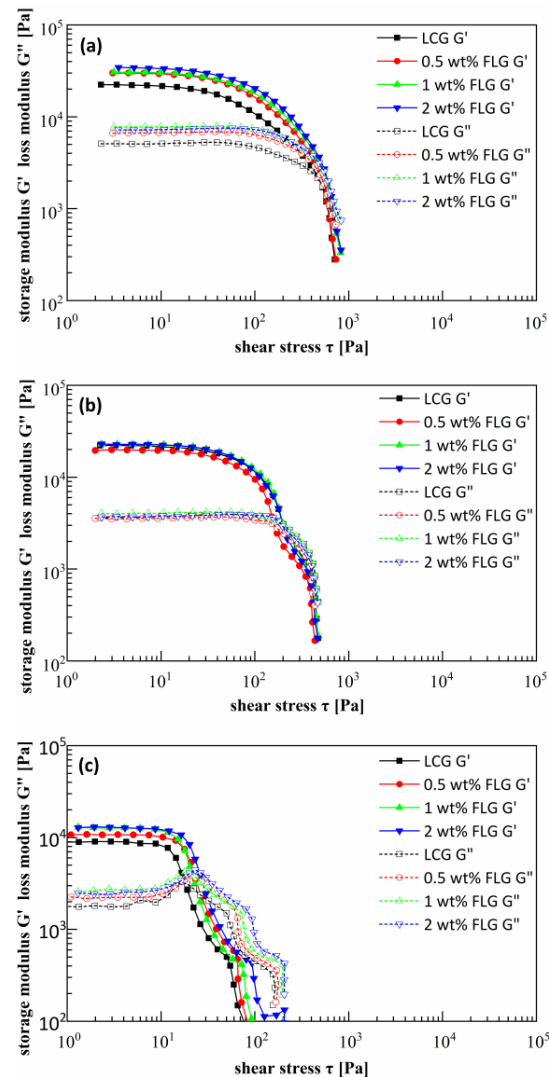


Figure 3. Changes in storage modulus G' and loss modulus G'' of LCG with shear stress. (a) 30 °C; (b) 70 °C; (c) 130 °C.

It can be seen from Figures 3 and 4 that the higher the FLG content, the greater the storage modulus and loss modulus of LCG, and the dynamic yield stress and the cross stress also increased to varying degrees, which shows that FLG additives can enhance the elasticity and viscosity of LCG. Combined with the microscopic morphological examination, FLG increases the density of the LCG fiber structure and increases the ability of the grease to resist elastic deformation and viscous flow. The higher the temperature, the smaller the storage modulus and loss modulus of LCG, and the greater the reduction in loss modulus, which shows that temperature will reduce the elasticity and viscosity of LCG, and has a greater impact on viscosity. The dynamic yield stress and cross stress of the LCG also decrease with the increase in temperature, which is related to the Brownian motion of the molecules. The higher the temperature, the more intense the Brownian motion of the molecules and the smaller the intermolecular force, which leads to easier yielding of the structure of the LCG and stronger fluidity. According to Figure 4, as a whole, the more FLG content, the greater the dynamic yield stress. However, the cross stress only shows this trend at 30 °C. Under the influence of a temperature rise, the effect of FLG on the cross stress is weakened. Comparing the effects of FLG addition and temperature changes on the dynamic yield stress and cross stress, it is found that FLG has a greater impact on the dynamic yield stress, and temperature changes have a greater impact on the cross stress. It can be proved that FLG mainly affects the elasticity of LCG, and temperature mainly affects the viscosity of LCG. Furthermore, adding an appropriate amount of FLG can offset the effect of temperature on the elasticity and viscosity of the LCG, which means that FLG additives can improve the viscosity-temperature performance of the grease and the elastic deformation with temperature.

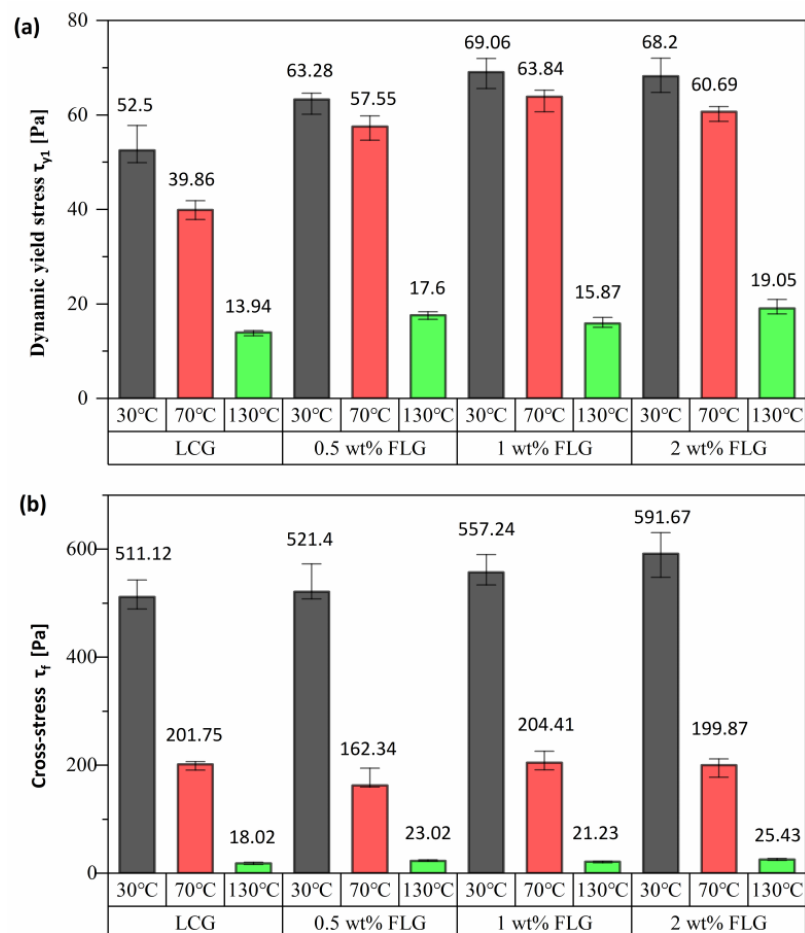


Figure 4. Dynamic yield stress and cross-stress of LCG. (a) Dynamic yield stress; (b) Cross-stress.

Figure 5 shows the variation in the shear stress versus the shear strain rate of the four greases at three temperatures, respectively: the shear strength (τ_y) of the four greases increases with the increase in the shear strain rate ($\dot{\gamma}$), indicating a non-linear trend. The regions of increasing shear stress are labeled a, c and e in Figure 5a, and a and c in Figure 5b,c. However, in area d (Figure 5a) and area b (Figure 5b,c), the increase in shear stress is much smaller than the overall growth trend, and this area is the shear yield area. The point where the shear stress begins to plateau is the yield point. Since the rotation mode is a steady state test, the corresponding shear stress is the steady state yield stress τ_{y2} . The steady-state yield stresses of the four LCGs at the three temperatures are given in Figure 6. In area b (Figure 5a), the shear stress tends to decrease (this area is the wall sliding area). The intermolecular resistance fails under the action of the external force and relative movement occurs between the molecular layers, and the ability of the LCG to resist deformation is weakened. Therefore, the measured shear stress begins to decrease, and the shear stress continues to increase until the wall-slip effect ends.

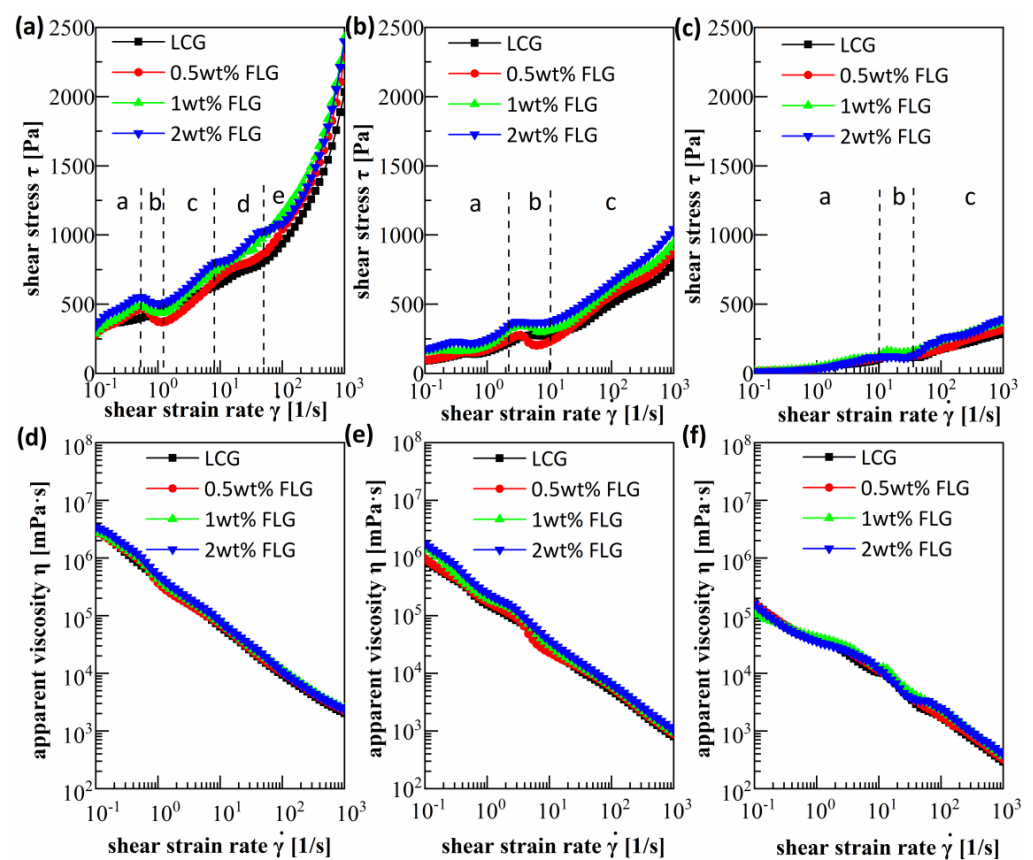


Figure 5. LCG shear stress and apparent viscosity curve: (a–c) shear stress; (d–f) apparent viscosity; (a,d) 30 °C; (b,e) 70 °C; (c,f) 130 °C.

According to Figure 5, it is found that at different temperatures, the higher the FLG content, the larger the shear stress borne by the LCG. It can be seen from Figure 2 that an increase in the amount of FLG can result in a denser microstructure of the LCG thickener and an increase in structural strength, resulting in an increase in the shear stress of the LCG as the amount of FLG increases. Through comparison of the data pertaining to each of two temperatures in Figure 5, it is found that with the increase in the shear strain rate, the shear stress of the LCG has a very obvious rising trend at 30 °C, the rising trend at 70 °C is relatively gentle, and the rising trend at 130 °C is more gentle. This means that the higher the temperature, the lower the rate at which the shear stress increases with the shear strain rate, and the lower the shear stress of the LCG. From the perspective of the influence of the

viscoelasticity on shear stress, the addition of FLG is shown to increase the viscoelasticity of LCG, and an increase in the temperature will reduce its viscoelasticity.

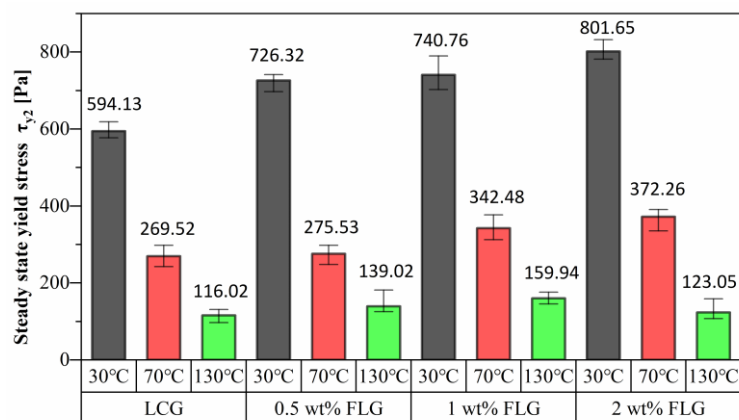


Figure 6. Steady state yield stress of LCG.

Comparing the yield zone of the LCG at different temperatures in Figure 5, combined with the steady-state yield stress data of Figure 6, it can be found that the steady-state yield stress of the same LCG is smaller at higher temperatures. Table 1 shows the effect of the FLG content on the steady-state yield stress of LCG. The steady-state yield stress of LCG with FLG contents of 0.5, one, and two is found to be increased by 22.25%, 24.68%, and 34.93%, respectively, at 30 °C compared with the LCG without FLG; the steady-state yield stress at 70 °C is increased by 2.23%, 27.07%, and 38.12%, respectively; the steady-state yield stress at 130 °C is increased by 19.82%, 38.86%, and 6.06%, respectively. On the whole, the addition of FLG at 70 °C increases the steady-state yield stress of LCG more significantly, indicating that among the three temperatures selected in the experiment, 70 °C is more suitable for FLG to play a role. And it shows that FLG additives can inhibit the temperature decrease in the yield strength of LCG.

Table 1. Steady state yield stress(τ_{y2}) of LCG at different FLG contents and temperatures.

T [°C]	LCG	0.5 wt% FLG		1 wt% FLG		2 wt% FLG	
	τ_{y2} [Pa]	τ_{y2} [Pa]	growth rate [%]	τ_{y2} [Pa]	growth rate [%]	τ_{y2} [Pa]	growth rate [%]
30	594.13	726.32	22.25	740.76	24.68	801.65	34.93
70	269.52	275.53	2.23	342.48	27.07	372.26	38.12
130	116.02	139.02	19.82	159.94	37.86	123.05	6.06

Viscosity is a characteristic of a substance that produces flow and irreversible deformation under stress. The apparent viscosity (η) is the ratio of the shear stress to the shear strain rate under steady flow. Figure 5a–c illustrates the changes in the apparent viscosity of the four greases with shear strain rate at different temperatures. The apparent viscosity of the four LCGs decreases with the increase in the shear strain rate, showing the phenomenon of shear thinning. This arises as some of the thickener fibers constituting the skeletal structure are oriented and unwound along the shear direction under the action of mechanical external forces, the skeleton is gradually destroyed and the shear resistance is reduced. According to Figure 5d–f, it is found that the higher the FLG content, the greater the apparent viscosity of the LCG; the higher the temperature, the lower the apparent viscosity of the LCG. This is due to the FLG additives densifying the structure of the LCG, resulting in an increase in flow resistance, which results in an increase in the apparent viscosity of the LCG. The higher the temperature, the more intense the Brownian motion of the molecules and the smaller the intermolecular forces, resulting in lower flow resistance, resulting in a decrease in the apparent viscosity of the LCG.

3.3. Effect of FLG on the Friction and Wear of LCG

The friction test used the SRV-4 friction test machine, which is lubricated with LCG containing 0 wt%, 0.5 wt%, 1 wt%, and 2 wt% FLG. The upper and lower friction pairs are made of GCr15 bearing steel. The test temperature was set to 30 °C, the load was 90N, the frequency was 10 Hz, and the amplitude was four mm. The test duration is 1800s.

Figure 7 shows the influence of FLG contents (0 wt%, 0.5 wt%, 1 wt%, and 2 wt%) on the friction curve of LCG. It can be seen that the friction curves of the LCG with FLG added are generally smaller than those of the LCG without FLG, and the friction curves of the LCG with a FLG content of 0.5 wt% are the smallest overall. The friction coefficients of the four LCG reached about 0.18 at 40 s, and then different contents of FLG began to work independently. Among them, LCG without FLG gradually formed the boundary film at 40 s, and the friction coefficient curve was relatively stable. At 220s, the boundary film gradually failed, the friction coefficient began to rise, and the friction coefficient reached about 0.2 at 320s. Then, the friction coefficient decreased slightly, indicating that the residual boundary film was still in effect, and a new boundary film was gradually formed. However, at 480s, the friction coefficient increased sharply to 0.23, and continued until the end of the friction experiment. At this moment, boundary lubrication is gradually formed. For LCG with a FLG content of 0.5 wt%, the friction curve fluctuates greatly from 40s to 160s. During this process, the disordered FLG in the LCG gradually becomes ordered under the action of the tangential force, and the boundary film is gradually formed. Then the friction curve fluctuated regularly and had a slight downward trend until the end of the friction experiment. This shows that under the action of 0.5 wt% FLG, the boundary film is more stable and can withstand longer friction without failure. The friction curve of LCG with a FLG content of 1 wt% did not fluctuate much from 40 s to the end of the test, and only fluctuated significantly between 900 s and 1000 s, indicating that 1 wt% of FLG also made the boundary film more stable. However, due to the increase in FLG content, the frictional resistance increases, resulting in the overall friction coefficient greater than that of LCG with FLG content of 0.5 wt%. LCG with a FLG content of 2 wt% began to fluctuate greatly at 40 s, and until 330 s, the friction coefficient gradually increased to about 0.21, and the effect of excessive FLG began to appear. From 330 s to the end of the test, the friction curve has been in a state of irregular fluctuation. This is due to the FLG content being too large and it is easy to agglomerate, however, under the action of the tangential force, the FLG has a tendency to change to an orderly state. FLG changes continuously in two states of agglomeration and order (as shown in Figure 8), so the friction curve fluctuates more obviously.

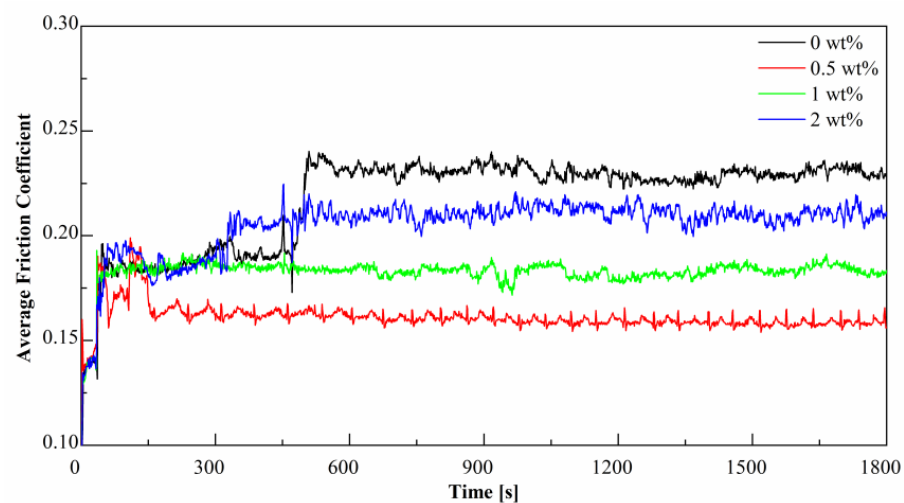


Figure 7. Average COF curve of LCG.

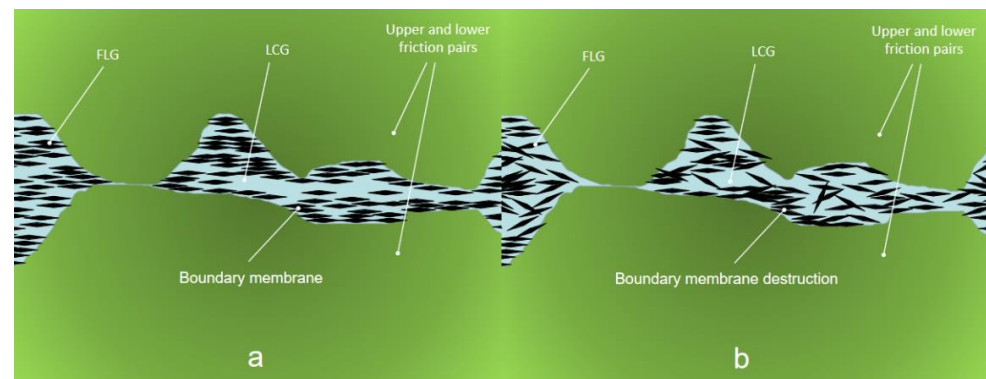


Figure 8. Two states of FLG in LCG: (a) Ordered arrangement; (b) Unordered aggregation.

Figure 9 shows the average wear scar diameter (WSD) and average friction coefficient (COF) for the four greases. It can be seen that the average WSD and average COF of LCG without FLG addition are the largest, and the average WSD and average COF of LCG with 0.5 wt% FLG content are the smallest. Figure 10 presents all the wear spot pictures of the four LCG, where Figure 10a–c are LCG, Figure 10d–f are LCG with 0.5 wt% FLG content, and Figure 10g–i are LCG with a FLG content of 1 wt%, Figure 10j–l are LCG with a FLG content of 2 wt%. According to Tables 2 and 3, LCG with a FLG content of 0.5 wt% has an increase of 52.05% in anti-friction ability and 19.60% in anti-friction ability compared with LCG without FLG. The LCG with a FLG content of 1 wt% increased the wear reduction ability by 16.06% and the anti-friction ability by 14.56%. The LCG with a FLG content of 2 wt% increased the wear reduction ability by 5.96% and the anti-friction ability by 7.09%. This shows that among the four selected lubricating greases, LCG with a FLG content of 0.5 wt% has the best anti-wear and anti-friction effect.

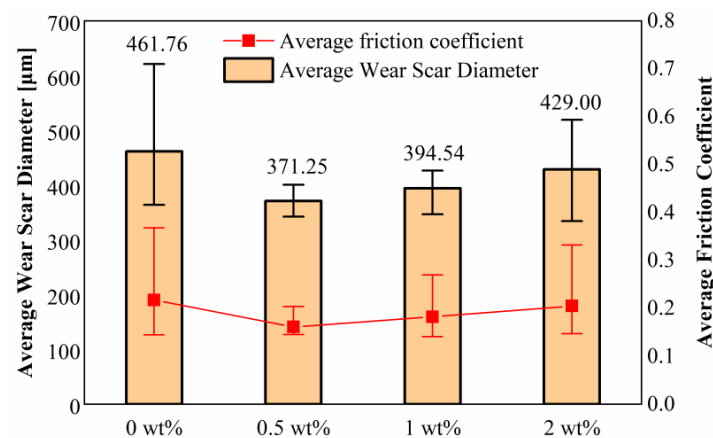


Figure 9. Average WSD and Average COF of LCG.

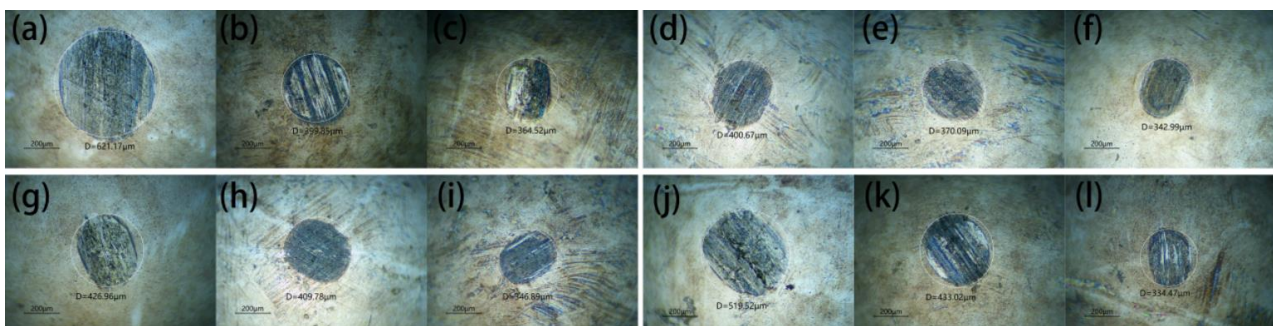


Figure 10. WSD of LCG: (a–c) LCG; (d–f) 0.5 wt% FLG; (g–i) 1 wt% FLG; (j–l) 2 wt% FLG.

Table 2. Average COF of LCG with different FLG contents.

LCG		0.5 wt% FLG		1 wt% FLG		2 wt% FLG	
COF [1]	COF [1]	Reduction Rate [%]	COF [1]	Reduction Rate [%]	COF [1]	Reduction Rate [%]	Reduction Rate [%]
0.218	0.161	52.05	0.183	16.06	0.205	5.96	

Table 3. Average WSD of LCG with different FLG contents.

LCG		0.5 wt% FLG		1 wt% FLG		2 wt% FLG	
WSD [μm]	WSD [μm]	Reduction Rate [%]	WSD [μm]	Reduction Rate [%]	WSD [μm]	Reduction Rate [%]	Reduction Rate [%]
461.76	371.25	19.60	394.54	14.56	429.00	7.09	

The wear volume of the steel ball was estimated once the height of the worn cap, h , was obtained by the following formula [23]:

$$h = r - \sqrt{r^2 - \frac{d^2}{4}} \quad (2)$$

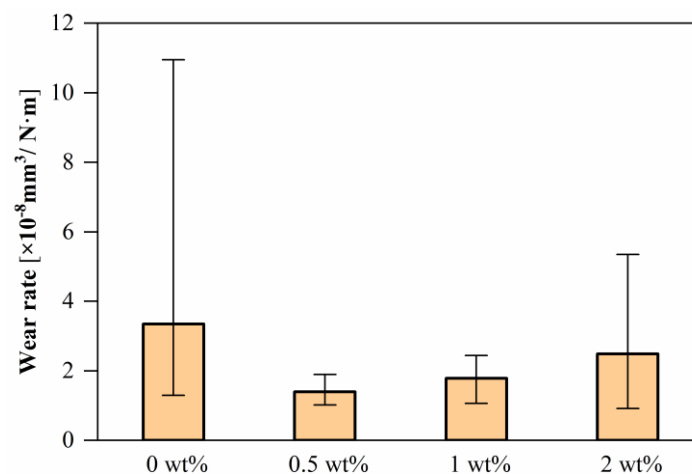
$$V = \left(\frac{\pi h}{6}\right) \left(\frac{3d^2}{4} + h^2\right) \quad (3)$$

where r is the initial radius of the ball and d is WSD. The specific wear rate can be defined as the volume of material removed per unit load and sliding distance:

$$W = \frac{V}{P \cdot S} \quad (4)$$

where V is the calculated wear volume, P is the applied normal load, and S is the total sliding distance.

Figure 11 shows a histogram of the average wear rates for the four greases. It can be seen that the wear rate trends of the four greases are the same as those of their WSD and COF.

**Figure 11.** Wear rate of steel balls.

The above phenomenon shows that, for LCG without FLG, the boundary film that gradually formed during the friction process can reduce friction, yet is easily destroyed, resulting in relatively large wear. When the FLG content is too high, FLG can fully cover

the friction surface, however, it is easy to polymerize during the friction process, so that the FLG changes continuously in the two states of disordered polymerization and ordered arrangement, which affects the anti-wear and anti-friction effect of the grease. Under the working conditions of this paper, the grease with FLG content of 0.5 wt% is the grease with the best friction and wear performance among the four greases.

4. Conclusions

1. The addition of FLG makes the fiber microstructure of the LCG more compact, resulting in greater structural strength, yield strength, apparent viscosity, storage modulus, and loss modulus of the LCG.
2. FLG can enhance the viscoelasticity of the LCG, and the increase in temperature will reduce the viscoelasticity of the LCG, and has a greater impact on the viscosity. Adding an appropriate amount of FLG can offset the effect of temperature on the elasticity and viscosity of the LCG, which means that FLG additives can improve the viscosity–temperature performance of the grease and the performance of the elastic deformation with temperature changes. Among the temperatures selected in this article, 70 °C is more suitable for FLG to play a role.
3. An appropriate amount of FLG can make the boundary film more stable, can withstand long-term friction without failure, and reduce wear. When the FLG content is too high, FLG can fully cover the friction surface, however, it is easy to polymerize during the friction process, which makes the FLG change continuously in the two states of disordered polymerization and ordered arrangement, resulting in the instability of the boundary film and affecting the friction effect. Under the working conditions of this paper, the grease with FLG content of 0.5 wt% is the grease with the best friction and wear performance among the four greases.

Author Contributions: Conceptualization, Y.W. and X.G.; methodology, Y.W.; software, X.G. and P.Z.; validation, Y.W., X.G. and P.Z.; formal analysis, Y.W., X.G. and P.Z.; investigation, X.G. and P.Z.; resources, Y.W. and J.L.; data curation, Y.W., X.G. and P.Z.; writing—original draft preparation, X.G. and P.Z.; writing—review and editing, Y.W. and J.L.; visualization, X.G.; supervision, Y.W. and J.L.; project administration, Y.W.; funding acquisition, Y.W. All authors have read and agreed to the published version of the manuscript.

Funding: This research was funded by National Natural Science Foundation of China (Grant No. 52075274 and 51475143) and Shandong Provincial Key Research and Development Program (Major Science and Technology Innovation Project) (Grant No. 2020CXGC011003).

Institutional Review Board Statement: Not applicable.

Informed Consent Statement: Not applicable.

Conflicts of Interest: The authors declare no conflict of interest.

Abbreviations

FLG	few-layer graphene
COF	friction coefficient
LCG	lithium complex grease
WSD	wear scar diameter
SEM	scanning electron microscope

References

1. Ma, S.; Zhang, X.; Yan, K.; Zhu, Y.; Hong, J. A Study on Bearing Dynamic Features under the Condition of Multiball–Cage Collision. *Lubricants*. **2022**, *10*, 9. [[CrossRef](#)]
2. Zhang, E.; Li, W.; Zhao, G.; Wang, Z.; Wang, X. A Study on Microstructure, Friction and Rheology of Four Lithium Greases Formulated with Four Different Base Oils. *Tribol. Lett.* **2021**, *69*, 98. [[CrossRef](#)]
3. Fan, X.; Li, W.; Li, H.; Zhu, M.; Xia, Y.; Wang, J. Probing the effect of thickener on tribological properties of lubricating greases. *Tribol. Int.* **2018**, *118*, 128–139. [[CrossRef](#)]

4. Kumar, N.; Saini, V.; Bijwe, J. Exploration of Talc nanoparticles to enhance the performance of Lithium grease. *Tribol. Int.* **2021**, *162*, 107107. [[CrossRef](#)]
5. Kumar, N.; Saini, V.; Bijwe, J. Performance properties of lithium greases with PTFE particles as additive: Controlling parameter-size or shape? *Tribol. Int.* **2020**, *148*, 106302. [[CrossRef](#)]
6. Huang, X.; Zhi, C.; Lin, Y.; Bao, H.; Wu, G.; Jiang, P.; Mai, Y.W. Thermal conductivity of graphene-based polymer nanocomposites. *Mater. Sci. Eng. R-Rep.* **2020**, *142*, 100577. [[CrossRef](#)]
7. Wu, W.; Chen, R.; Yang, Z.; He, Z.; Zhou, Y.; Lv, F. Corrosion resistance of 45 carbon steel enhanced by laser graphene-based coating. *Diam. Relat. Mat.* **2021**, *116*, 108370. [[CrossRef](#)]
8. Mao, J.; Chen, G.; Zhao, J.; He, Y.; Luo, J. An investigation on the tribological behaviors of steel/copper and steel/steel friction pairs via lubrication with a graphene additive. *Friction* **2021**, *9*, 228–238. [[CrossRef](#)]
9. Niu, M.; Qu, J.; Gu, L. Synthesis of titanium complex grease and effects of graphene on its tribological properties. *Tribol. Int.* **2019**, *140*, 105815. [[CrossRef](#)]
10. Wang, J.; Guo, X.; He, Y.; Jiang, M.; Gu, K. Tribological characteristics of graphene as grease additive under different contact forms. *Tribol. Int.* **2018**, *127*, 457–469. [[CrossRef](#)]
11. Zhao, J.; Huang, Y.; Li, Y.; Gao, T.; Dou, Z.; Mao, J.; Wang, H.; He, Y.; Li, S.; Luo, J. Superhigh-exfoliation graphene with a unique two-dimensional (2D) microstructure for lubrication application. *Appl. Surf. Sci.* **2020**, *513*, 145608. [[CrossRef](#)]
12. Curà, F.; Mura, A.; Adamo, F. Experimental investigation about tribological performance of graphene-nanoplatelets as additive for lubricants. *Procedia Struct. Integr.* **2018**, *12*, 44–51. [[CrossRef](#)]
13. Zheng, D.; Cai, Z.; Shen, M.; Li, Z.; Zhu, M. Investigation of the tribology behaviour of the graphene nanosheets as oil additives on textured alloy cast iron surface. *Appl. Surf. Sci.* **2016**, *387*, 66–75. [[CrossRef](#)]
14. Wu, L.; Gu, L.; Jian, R. Lubrication mechanism of graphene nanoplates as oil additives for ceramics/steel sliding components. *Ceram. Int.* **2021**, *47*, 16935–16942. [[CrossRef](#)]
15. Radhika, P.; Sobhan, C.B.; Chakravorti, S. Improved tribological behavior of lubricating oil dispersed with hybrid nanoparticles of functionalized carbon spheres and graphene nano platelets. *Appl. Surf. Sci.* **2021**, *540*, 148402. [[CrossRef](#)]
16. Wang, W.; Zhang, G.; Xie, G. Ultralow concentration of graphene oxide nanosheets as oil-based lubricant additives. *Appl. Surf. Sci.* **2019**, *498*, 143683. [[CrossRef](#)]
17. Ouyang, T.; Shen, Y.; Lei, W.; Xu, X.; Liang, L.; Waqar, H.S.; Lin, B.; Tian, Z.; Shen, P. Reduced friction and wear enabled by arc-discharge method-prepared 3D graphene as oil additive under variable loads and speeds. *Wear* **2020**, *462*, 203495. [[CrossRef](#)]
18. Mohamed, A.; Tirth, V.; Kamel, B.M. Tribological characterization and rheology of hybrid calcium grease with graphene nanosheets and multi-walled carbon nanotubes as additives. *J. Mater. Res. Technol.* **2020**, *9*, 6178–6185. [[CrossRef](#)]
19. Li, Z.; He, Q.; Du, S.; Zhang, Y. Effect of few layer graphene additive on the tribological properties of lithium grease. *Lubr. Sci.* **2020**, *32*, 333–343. [[CrossRef](#)]
20. Zhang, J.; Wang, A.; Yin, H. Preparation of graphite nanosheets in different solvents by sand milling and their enhancement on tribological properties of lithium-based grease. *Chin. J. Chem. Eng.* **2020**, *28*, 1177–1186. [[CrossRef](#)]
21. Ouyang, T.; Shen, Y.; Yang, R.; Liang, L.; Liang, H.; Lin, B.; Tian, Z.; Shen, P. 3D hierarchical porous graphene nanosheets as an efficient grease additive to reduce wear and friction under heavy-load conditions. *Tribol. Int.* **2020**, *144*, 106118. [[CrossRef](#)]
22. Aziev, R.; Savilov, S.; Kupreenko, S.; Ivanov, A.; Stolbov, D.; Usol'tseva, N.; Lunin, V. Graphene nanoflakes as effective dopant to Li-based greases. *Funct. Mater. Lett.* **2020**, *9*, 2040006. [[CrossRef](#)]
23. Lin, B.; Rustamov, I.; Zhang, L.; Luo, J.Q.; Wan, X. Graphene-Reinforced Lithium Grease for Antifriction and Antiwear. *ACS Appl. Nano Mater.* **2020**, *3*, 10508–10521. [[CrossRef](#)]
24. Jin, B.; Zhao, J.; Chen, G.; He, Y.; Huang, Y.; Luo, J. In situ synthesis of Mn₃O₄/graphene nanocomposite and its application as a lubrication additive at high temperatures. *Appl. Surf. Sci.* **2021**, *546*, 149019. [[CrossRef](#)]
25. Liu, X.; Chen, H.; Qiao, D.; Feng, D.; Wang, H.; Meng, W. The Influence of Graphene Oxide on the Tribological Properties of Lithium-based Grease. *Sur. Tech.* **2021**, *50*, 70–78. [[CrossRef](#)]
26. Sun, Z.; Xu, C.; Peng, Y.; Shi, Y.; Zhang, Y. Fretting tribological behaviors of steel wires under lubricating grease with compound additives of graphene and graphite. *Wear* **2020**, *454*, 203333. [[CrossRef](#)]
27. Cheng, Z.; Kong, Y.; Fan, L.; Liu, Z. Ultrasound-assisted Li⁺/Na⁺ co-intercalated exfoliation of graphite into few-layer graphene. *Ultrason. Sonochem.* **2020**, *66*, 105108. [[CrossRef](#)]
28. Pan, J.; Cheng, Y.; Qian, M.; Zhou, B. Thermal-rheological properties and variation mechanisms of lithium lubricating grease. *Chem. Ind. Eng. Progress* **2018**, *37*, 1509–1515. [[CrossRef](#)]